

Role of metal ions in catalysis by HIV integrase analyzed using a quantitative PCR disintegration assay

Tracy L. Diamond and Frederic D. Bushman*

Department of Microbiology, University of Pennsylvania School of Medicine, 3610 Hamilton Walk Philadelphia, PA 19104-6076, USA

Received July 27, 2006; Revised September 29, 2006; Accepted October 3, 2006

ABSTRACT

Paired metal ions have been proposed to be central to the catalytic mechanisms of RNase H nucleases, bacterial transposases, Holliday junction resolvases, retroviral integrases and many other enzymes. Here we present a sensitive assay for DNA transesterification in which catalysis by human immunodeficiency virus-type 1 (HIV-1) integrase (IN) connects two DNA strands (disintegration reaction), allowing detection using quantitative PCR (qPCR). We present evidence suggesting that the three acidic residues of the IN active site function through metal binding using metal rescue. In this method, the catalytic acidic residues were each substituted with cysteines. Mn^{2+} binds tightly to the sulfur atoms of the cysteine residues, but Mg^{2+} does not. We found that Mn^{2+} , but not Mg^{2+} , could rescue catalysis of each cysteine-substituted enzyme, providing evidence for functionally important metal binding by all three residues. We also used the PCR-booster assay to show that HIV-1 IN could carry out transesterification reactions involving DNA 5' hydroxyl groups as well as 3' hydroxyls as nucleophiles. Lastly, we show that Mn^{2+} by itself (i.e. without enzyme) can catalyze formation of a low level of PCR-amplifiable product under extreme conditions, allowing us to estimate the rate enhancement due to the IN-protein scaffold as at least 60 million-fold.

INTRODUCTION

Divalent metal ions are required for catalysis by many enzymes that carry out nucleic acid phosphoryl-transfer reactions. It has been proposed for many such enzymes that rate enhancement is mostly due to metal–nucleic acid interactions in the transition state, and the role of the protein scaffold is mainly to bind and position the metal ions and substrates

(1,2). This may explain the ability of dissimilar metal binding protein and RNA enzymes to carry out related chemical reactions (3–5).

The role of bound metals has been studied extensively for members of the ribonuclease H (RNase H)-like enzyme superfamily, which includes RuvC resolvase, bacterial and retroviral RNase Hs, bacterial transposases and retroviral integrases, all of which carry out polynucleotide phosphoryl-transferase reactions. These enzymes have similar secondary structures within their catalytic domains. The protein folds bring together three or four conserved acidic residues that are thought to be involved in metal coordination (4–7). These enzymes can utilize Mn^{2+} and/or Mg^{2+} for catalysis, though other metal ions can bind and for some enzymes support partial function (8–12).

Three hypotheses for metal binding by RNase H-like enzymes have been proposed. Several RNase H enzyme structures determined by X-ray crystallography have been shown to contain two metal atoms bound at the active site (12–14), but the majority of structures have only one bound metal (9,15–19). The latter observation supports the second hypothesis that only one metal is involved catalytically (16,20,21). However, observation of a single bound metal in the absence of substrate could reflect the need for nucleic acid substrate binding to stabilize metal binding at the second site. As a third possibility, it has also been proposed that two metals bind, with the first activating catalysis and the second inhibiting (22).

The human immunodeficiency virus (HIV) integrase (IN) is a member of the RNase H-like superfamily and has been extensively studied for metal binding at the D₁DX₃₅E motif (composed of D64, D116 and E152). Several structural studies of retroviral INs in the absence of DNA substrate have reported binding of a single Mg^{2+} ion between the two aspartate residues (8,17,18), but none have shown Mg^{2+} binding at the second site between residues D64 and E152. Crystal structures of the avian sarcoma virus (ASV) IN in the presence of Cd^{2+} or Zn^{2+} ions revealed two bound metals at the catalytic triad (8). However, these complexes did not retain normal catalytic activity, complicating interpretation.

*To whom correspondence should be addressed. Tel: +1 215 573 8732; Fax: +1 215 573 4856; Email: bushman@mail.med.upenn.edu

In a previous study, binding of divalent metal ions by the HIV-1 IN catalytic triad was investigated using metal rescue of cysteine substitutions (23). The metal rescue technique has been used to map metal binding sites for ribozymes, such as the Tetrahymena group I ribozyme or the human spliceosome (24–27) and protein enzymes, such as NAD-dependent isocitrate dehydrogenase, *Escherichia coli* DNA polymerase I and RNase H-like enzyme superfamily members (28–33). Metal rescue takes advantage of the unique property of Mn^{2+} to bind tightly to sulfur atoms, while Mg^{2+} ions bind much more weakly. For analysis of ribozymes, sulfur substitutions have been carried out with oxygens in the substrate or nucleophile RNA, while for protein enzymes, suspected metal binding residues can be tested by replacement with cysteines. If the mutated motif has a necessary interaction with metal ions, then the enzyme will not be functional in reactions with Mg^{2+} , but may be functional in the presence of Mn^{2+} , indicating a requirement for metal binding. These assays have been used to analyze metal binding by HIV-1 IN, and indicated functional metal binding by residues D64 and D116, but did not show activity with either metal for E152C (23). It was unclear whether the absence of activity for the E152C IN was due to a lack of metal binding by that residue or a lack in assay sensitivity.

Here, we report an ultra-sensitive assay for measuring nucleic acid transesterification reactions *in vitro* and its use to investigate metal-mediated catalysis by HIV-1 IN. The assay is based on the HIV-1 IN disintegration reaction (34), which is a DNA transesterification reaction that reverses the normal integration reaction catalyzed by HIV-1 IN (Figure 1A, see legend for details). In disintegration, the 3' hydroxyl of the target DNA at the insertion site attacks the DNA backbone between the viral and target DNA, thereby joining the target DNA segments and releasing the viral LTR end. Similar activities have been reported for the RAG-1 recombinase involved in V(D)J recombination (35), and the Mu transposase (36). To boost the sensitivity, we developed lengthened disintegration substrates, which allowed PCR amplification and TaqMan detection (Figure 1B), which greatly increases sensitivity over previous assays.

We used this assay to probe three aspects of metal-mediated catalysis by HIV-1 IN. First, we demonstrate metal rescue for HIV-1 IN derivatives containing cysteine substitutions at all three residues of the catalytic triad, including E152. These studies established that two metal ions are likely involved in catalysis and support the idea that this is generally true for the retroviral INs. Second, we used this assay to measure DNA transesterification reactions on a related substrate with a 5' hydroxyl functioning as the nucleophile instead of a 3' hydroxyl. We found that HIV-1 IN was able to catalyze transesterification at a low level on this substrate as well, but was more selective for metal ion usage than seen for the standard substrate. In the third application, we took advantage of the exceptional sensitivity of the assay to detect transesterification in the presence of Mn^{2+} alone in the absence of a protein enzyme scaffold. This allowed us to estimate the rate enhancement contributed by binding of the metal and DNA substrate to the IN-protein scaffold as at least a factor of 60 million.

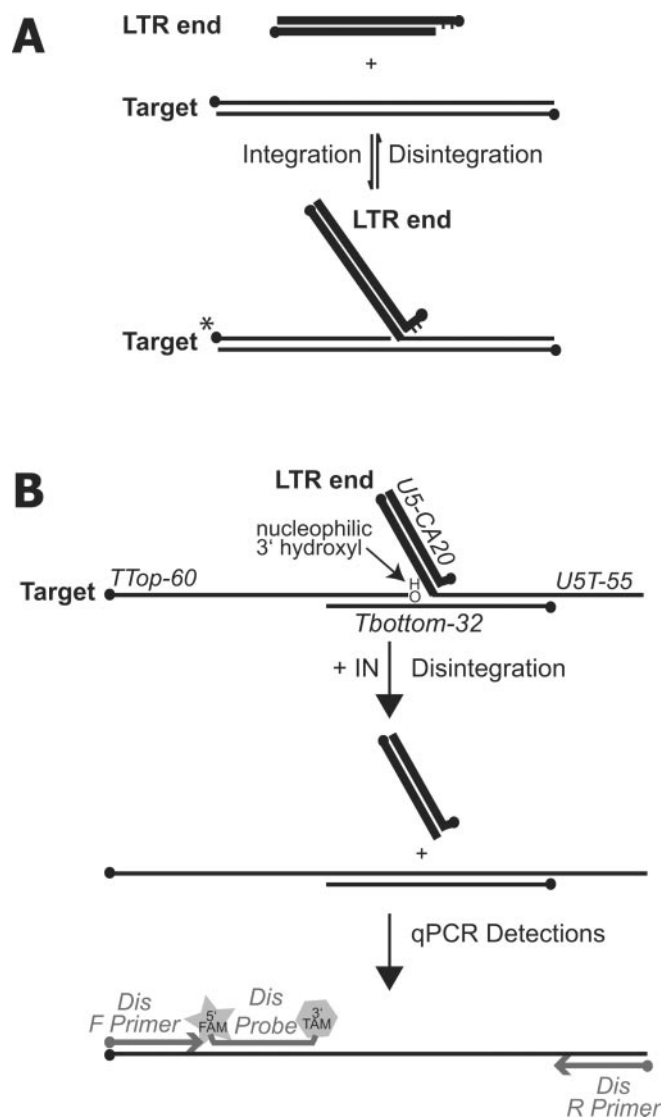


Figure 1. Disintegration and the PCR-based disintegration assay. (A) Diagram of integration and disintegration. During normal integration, IN first cleaves 2 nt off the 3' end of each LTR DNA. IN then catalyzes a coupled DNA breaking and joining reaction, which covalently joins the viral DNA 3' end to host cell DNA. Disintegration is the reversal of the integration reaction. In disintegration, the 3' end in the target DNA at the junction with the viral DNA attacks the nearby phosphodiester, rejoining the target DNA segment and releasing the viral DNA. For standard disintegration assays *in vitro*, a ^{32}P -radiolabel is attached at the indicated 5' end (*), allowing detection of the larger product formed by disintegration (34). (B) The qPCR-based disintegration assay. The assay substrate contains four annealed oligonucleotides resembling the integration product (upper). DNA transesterification can occur on this substrate, yielding the 97mer disintegration product (middle). The product can be quantitated by TaqMan qPCR (lower). Nucleic acid 5' ends are represented by black dots. LTR ends are represented by thick lines, while target is represented by thin lines.

MATERIALS AND METHODS

Enzymes

Protein expression vectors used encode IN derived from the NL4-3 strain of HIV-1 fused at the N-terminus to a hexahistidine tag and thrombin cleavage site. All vectors were generated using site-directed mutagenesis and were described

previously (23,37). The wild-type (WT) IN used contains the F185H solubility improving substitution.

Protein expression and purification was carried out as described previously for this vector (38). IN containing plasmid constructs were transformed into BL21-CodonPlus(DE3)-RIL *E.coli* cells (Stratagene), and protein expression was induced with 150 μ M isopropyl- β -D-thiogalactopyranoside (IPTG) at an OD₆₀₀ of 0.5. After 3 h at 37°C, cells were harvested and pellets were flash frozen in liquid nitrogen and stored at -80°C. Cell pellets from induced cultures were resuspended in lysis buffer [20 mM Tris-HCl (pH 7.9) and 200 mM NaCl] and lysed with 2 mg/ml lysozyme. Proteinase inhibitor cocktail I (1 \times ; Calbiochem) and 10 mM CHAPS (Sigma-Aldrich) were added, and the solution was brought to 1 M NaCl, 5 mM β -mercaptoethanol (β -ME) and 5 mM imidazole. The lysate was then sonicated and cleared by centrifugation and passage through a 0.45 μ m filter. The sample was loaded onto a Ni-nitrilotriacetic acid agarose resin (Invitrogen) that was previously equilibrated with binding buffer [1 M NaCl, 20 mM Tris-HCl (pH 7.9), 5 mM β -ME, 10 mM CHAPS and 10 mM imidazole]. The column was washed with binding buffer and wash buffer [1 M NaCl, 20 mM Tris-HCl (pH 7.0), 5 mM β -ME, 10 mM CHAPS and 25 mM imidazole]. Finally, the column was eluted with elution buffer [1 M NaCl, 20 mM Tris-HCl, 5 mM β -ME, 10 mM CHAPS and 0.2 M imidazole], and buffer exchange was carried out using a YM-30 Centriprep (Millipore) to transfer the protein into IN storage buffer [ISB; 20% glycerol, 727 mM NaCl, 7.27 mM HEPES (pH 7.5), 7.27 mM β -ME and 7.27 μ M ZnSO₄].

Oligonucleotides

All oligonucleotides were purchased from Integrated DNA Technologies. The PCR-boosted disintegration substrate (Figure 1B, top) consists of four oligonucleotides, U5CA-20 d(ACGTCTAGAGATTTCCACA), U5T-55 d(TGTGGAA AATCTCTAGCACATTCCTTATCCCACTAGCTCTCTCG-ACGCAGGACTC), TTop-60 d(GTGTGCCCGTCTGTTGTGTCTCTCAGTGGCGCCCGAACAGGGACACATTACTT-ATCTAC) and Tbottom-32 DNA d(AGTGGGATAAGGAA-TGGTAGATAAGTAATGTG) or Tbottom-32 RNA r(AGU-GGGUAUAGGAAUGGUAGUAUAGUUAUGUG). As seen in Figure 1B, the substrate encodes the viral U5 terminus (LTR end) and a region representing target DNA (target). Primers for product quantification are Dis F d(TGTGT-GCCCGTCTGTTGTGT), Dis R d(GAGTCCTGCGTCCGAGAGAC), and the TaqMan[®] Probe, Dis Probe [5'-FAM-d(CAGTGGCGCCCGAACAGGGA)-TAMNph-3']. A 97mer oligonucleotide, Dis Full-97 d(TGTGTGCCCGTCTGTTGTGTCTCTCAGTGGCGCCCGAACAGGGACACATTACTT-ATCTACCATTCTTATCCCACTAGCTCTCTCGACGCA-GGACTC), representing the expected disintegration product was used to generate a standard curve.

A 'reverse polarity' substrate (Figure 4A) was also constructed using Tbottom-32 RNA (see above), U5-18 d(TGTG-GAAAATCTCTAGCA), Ttop-37 d(CATTCCTTATCCCACTAGCTCTCTCGACGAGGACTC), and TU5-78 d(TGTGTGCCCGTCTGTTGTGTCTCTCAGTGGCGCCCGAACAGGGACACATTACTTATCTACTGCTAGAGATTTCC-ACA). Primers for product quantification are the same as those used for the standard substrate (Figure 1B, upper).

Substrates were made by mixing the constituent oligonucleotides at a concentration of 800 nM each in water (test reactions were performed with substrates annealed in 0.1 M NaCl and results were unchanged) and slow cooling from 95°C (all DNA substrates) or 65°C (RNA containing substrates) down to 4°C at a rate of 0.5°C per 1.5 min. For reaction containing radiolabeled substrate TTop-60 (see above) was 5' end-labeled with [γ -³²P]ATP using polynucleotide kinase. The radiolabeled oligonucleotide was then annealed to the other oligonucleotides as above. The annealed substrate was applied to a G50-microspin column to remove unincorporated [γ -³²P]ATP. For reactions with radiolabeled PCR primer, Dis F was 5' end-labeled with [γ -³²P]ATP using polynucleotide kinase and was then applied to a G50-microspin column to remove unincorporated [γ -³²P]ATP.

qPCR-based disintegration assay

Unless otherwise noted, reactions were carried out in 40 μ l total volume with 30 nM substrate, 19.8 μ M HEPES (pH 7.3), 1.8 mM β -ME, 10 mM MnCl₂ or 20 mM MgCl₂, and 1 μ M IN. Reactions were started by addition of 2 μ l 20 μ M IN (diluted in ISB). Reactions were incubated at 37°C for the indicated length of time and stopped by addition of 5 μ l of a solution of 4.5% SDS and 1.35 mg/ml Proteinase K (Roche Applied Science) and incubation at 37°C for an additional 45 min. Reactions were heated at 65°C for 5 min prior to purification via the QIAquick Nucleotide Removal Kit (Qiagen). DNA was eluted in the provided Buffer EB.

Reactions were quantified by real-time qPCR after dilution in Buffer EB to obtain DNA samples in the linear range. qPCR were carried out in 25 μ l total volumes on an ABI Prism 7700 (Applied Biosystems) using the TaqMan[®] Universal PCR Master Mix (Applied Biosystems), 300 nM each primer, 200 nM Late-RT-Probe. A total of 5 μ l of reaction sample or standard curve were added per reaction. The universal cycling conditions (50°C 2 min, 95°C 10 min, 40 cycles of 95°C 15 s and 60°C 1 min) recommended by Applied Biosystems were used.

Comparative reactions with ³²P-labeled substrate followed the same protocol for the transesterification portion of the qPCR-based disintegration assay and were stopped by addition of 200 μ l formamide loading buffer [80% (w/v) deionized formamide, 10 mM EDTA (pH 8.0), 1 mg/ml xylene cyanol FF and 1 mg/ml bromophenol blue] rather than by SDS/Proteinase K treatment and nucleotide removal kit. A total of 5 μ l of each reaction was applied to an 8% denaturing-polyacrylamide gel and analyzed using OptiQuant software on a Storm PhosphorImager (GE Healthcare).

Reactions quantified using ³²P-labeled Dis F primer were performed on 1000-fold dilutions of nucleotide removal kit purified transesterification reactions using the same conditions as for the qPCR analysis (no probe was added). PCR products were diluted 5-fold in formamide loading buffer (see above) and 5 μ l of each sample was analyzed by 8% denaturing-polyacrylamide gel as discussed above.

qPCR-based DNA transesterification reactions with metal only

These reactions, carried out in the absence of IN, followed the protocol discussed above. Reactions were carried out in

a 40 μ l total starting volume with 30 nM substrate, 19.8 μ M HEPES (pH 7.3), 1.8 mM β -ME and EDTA or metal at the indicated concentration. Reactions were dehydrated by SpeedVac without heating for 5 h, followed by heating of the dried pellet at 95°C for the indicated length of time. Dehydrated and/or heated reactions were resuspended in 40 μ l H₂O at room temperature for 5 min with periodic vortexing. Reactions were purified via the Qiaquick Nucleotide Purification Kit as discussed above for IN containing reactions. Analysis of reaction products via TaqMan qPCR or [γ -³²P]ATP labeled LRT F primer was performed as described above.

RESULTS

qPCR-based assay for disintegration

We developed a qPCR assay to boost the sensitivity for detecting disintegration (Figure 1B). In previous studies, disintegration assays were carried out using ³²P end-labeled oligonucleotides, with the label attached to the nicked target strand, so that disintegration generated a longer strand (Figure 1A, star). The longer DNA product strand could then be quantified using PhosphorImager analysis.

To increase the assay sensitivity, a substrate was designed composed of the four oligonucleotides indicated in Figure 1B, which annealed to form a DNA three-way junction. The

substrate models a single HIV-1 LTR end inserted into a target DNA. The target DNA has a 16 nt double-stranded region on either side of the LTR insertion and single-stranded extensions 5' and 3', which contain regions for the binding of primers and a TaqMan probe. The transesterification reaction involves attack of the free 3' hydroxyl on the phosphodiester between the LTR and target DNA segments, removing the LTR duplex and joining the target DNA to form a 97mer product. The 97mer product can be quantitated using TaqMan based qPCR.

A single-stranded oligonucleotide matching the 97mer disintegration product was synthesized and used to make a standard curve for quantitation of PCR products (see Figure 2A). Amplification of dilutions of the 97mer for standard curve generation yielded reproducible signals with correlation coefficients >0.99.

Our first substrate design using all DNA oligonucleotides was not successful. The amounts of apparent disintegration product detected using the qPCR-based disintegration assay were roughly 1000-fold less than the amount detected in identical reactions using end-labeled substrates analyzed by gel electrophoresis (data not shown). As one possible improvement, we substituted the bottom DNA strand (T_{bottom}-32) with an RNA strand of identical length and sequence, based on the idea that the T_{bottom}-32 strand inhibited elongation during PCR, and an RNA strand could be degraded by addition of RNase. Much higher levels of

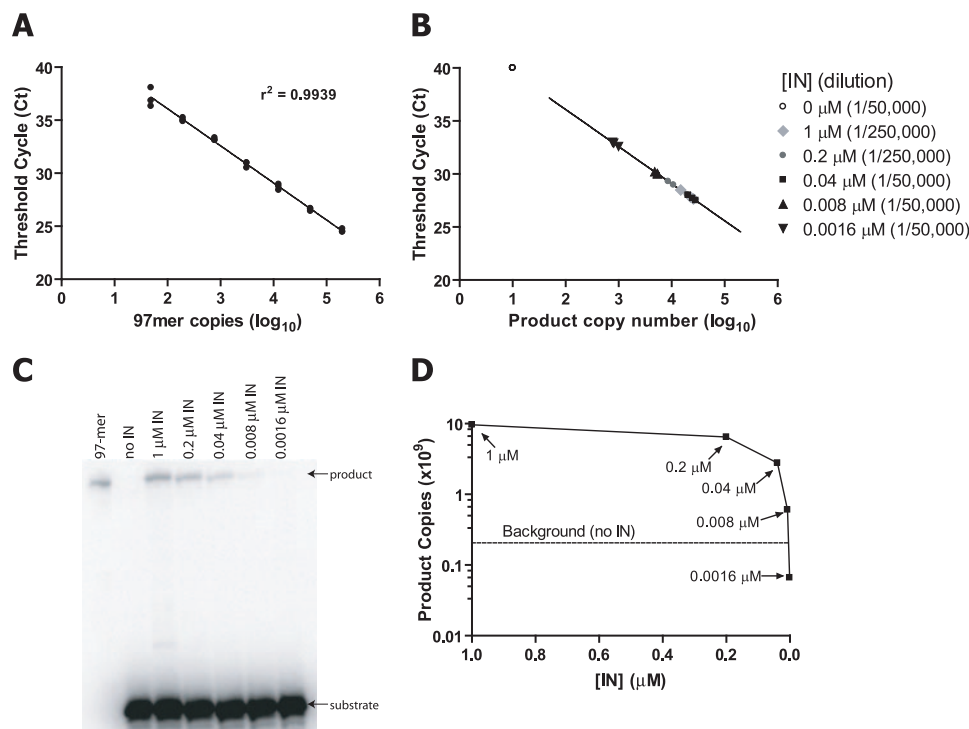


Figure 2. Sensitivity of the PCR-based disintegration assay. (A) A standard curve was generated using 4-fold dilutions of the synthetic 97mer product oligonucleotide (Dis Full-97). The standard curve was linear and reproducible in the range tested (from ~50 to 200 000 copies). (B) Disintegration reactions were carried out with dilutions of HIV-1 IN and analyzed in triplicate by qPCR. The IN reaction products were diluted by the factor shown. The threshold cycles for the IN reactions were compared to the standard curve for quantitation of product copies. (C) Disintegration reactions were carried out on a substrate with the T_{top}-60 oligonucleotide ³²P-labeled at the 5' end. Reactions were analyzed by 8% denaturing-polyacrylamide gel and PhosphorImager. (D) The total number product copies for reactions with radiolabeled substrate were calculated after measurement of percent product conversion at each IN concentration using ImageQuant software. Assay background was determined from the reaction with no IN added.

product were detected in the qPCR-based disintegration assay in reactions containing the RNA Tbottom-32 strand (data not shown). Subsequent experiments showed that it was not necessary to add RNase, possibly because the RNA strand was destroyed during thermocycling. Comparison of disintegration reactions using ^{32}P -labeled substrates with either RNA or DNA Tbottom-32 strands showed indistinguishable amounts of product formation, indicating that the RNA strand was influencing the PCR detection step and not the disintegration reaction itself (data not shown). The Tbottom-32 RNA strand was thus used in all subsequent assays.

In order to assess the sensitivity of the qPCR-based disintegration assay, we carried out disintegration reactions in the presence of decreasing concentrations of HIV-1 IN and quantified them using the qPCR and the ^{32}P methods. For the qPCR-based detection, reaction products were diluted up to 250 000-fold in order to obtain measurements in the linear range of the standard curve (Figure 2B). In our test reactions, the lowest concentration of IN used, 0.0016 μM , generated product that was well within the linear range, even at a 50 000-fold dilution. Reactions performed in the absence of IN did not yield product after 40 cycles of amplification.

Figure 2C displays products of transesterification reactions carried out using ^{32}P -labeled substrate and analyzed by 8% denaturing-PAGE. Product formation was detectable for the three highest concentrations of IN, but was less evident

with 0.08 μM or 0.0016 μM IN. The product size matched the labeled 97mer oligonucleotide marker as expected. The percent of substrate converted to product was measured using ImageQuant software and converted to the total number of product copies (Figure 2D). The dashed line in the graph represents background in the no IN control. The 0.008 μM IN reaction product is slightly above background, while the 0.0016 μM IN sample is below background. We have not made a specific effort to determine the lowest amount of product detectable using the qPCR-based assay. However, comparison of the product conversion measured under conditions of very low activity (see below) indicate that the qPCR-based disintegration assay is at least 1000-fold more sensitive than the ^{32}P -based assay.

Metal rescue analysis of cysteine substitutions in the HIV-1 IN active site

We examined the disintegration capabilities of HIV-1 IN variants containing alanine and cysteine substitutions within the conserved D,DX₃₅E catalytic triad in order to assess the role of metal binding in the active site (Figure 3). It has been hypothesized that the D64, D116 and E152 residues of HIV-1 IN coordinate two divalent metal ions (Figure 3A). The wild-type glutamate and aspartate amino acids are capable of binding both Mn^{2+} and Mg^{2+} . In contrast, cysteines can

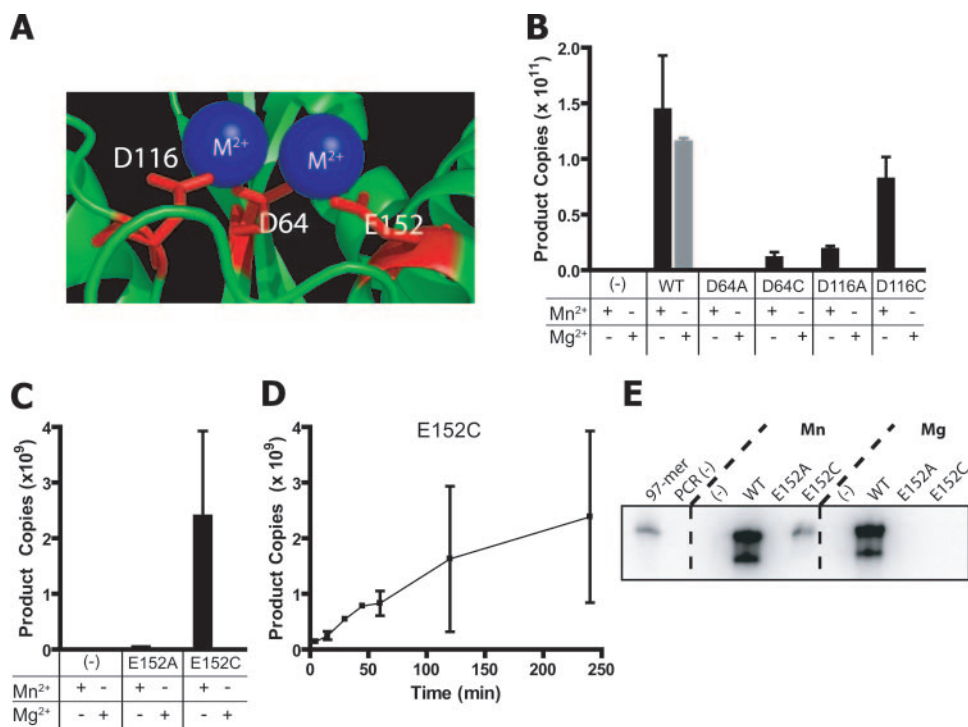


Figure 3. Functional metal binding by all three residues of the conserved D,DX₃₅E motif of HIV-1 IN. (A) Two divalent metal ions proposed to bind to the active site are shown interacting with the conserved acidic residues of HIV-1 IN. This model was adapted from the structure of avian sarcoma leukemia virus (1VSJ.pdb) in complex with cadmium ions (8). (B) Assays of WT IN and substitutions at D64 and D116. (C) Assays of substitutions at E152. PCR-based disintegration assays were carried out with the indicated IN derivatives in the presence of 10 mM Mn^{2+} or 20 mM Mg^{2+} . Disintegration reactions were incubated for 4 h at 37°C. The amount of product copies was determined using 250 000-fold dilutions of WT IN, 50 000-fold dilutions of D64 and D116 substituted INs and 10 000-fold dilutions or E152 substituted INs in the qPCR. The total product copies generated in the disintegration reaction is graphed. A one-tailed Mann-Whitney *U*-test was used to compare three independent disintegration reactions with qPCR in at least triplicate for each of the E152A and E152C Mn^{2+} reactions or the E152C Mn^{2+} and Mg^{2+} reactions to show that the difference between the sets was statistically significant with $P < 0.0001$. (D) A time course for disintegration activity with E152C IN. All error bars indicate one standard deviation around the mean of qPCR performed in triplicate. (E) Verification of the sizes of disintegration reaction products by PCR amplification and end labeling.

bind tightly to Mn^{2+} , but not to Mg^{2+} . Cysteine-substituted INs that are functional in the presence of Mn^{2+} , but not Mg^{2+} , reveal amino acids that interact directly with metal ions during enzyme catalysis. Alanine can not bind either divalent metal ion, so alanine substitutions serve as negative controls.

In these studies, we analyzed the disintegration activity in the presence of 10 mM MnCl_2 or 20 mM MgCl_2 . These metal concentrations were chosen because they showed the highest amount of product conversion during metal titration experiments with wild-type (WT) IN (data not shown). As seen in Figure 3B, WT IN was able to convert $1.44 \pm 0.49 (\times 10^{11})$ copies of substrate to product using Mn^{2+} as the coordinating metal ion during a 4 h disintegration reaction. At optimized metal concentrations, activity in the presence of Mg^{2+} was 20% lower than in the presence of Mn^{2+} . The initial rate of product formation was estimated at $51.03 \pm 7.47 (\times 10^{-6})$ product copies generated per minute per molecule IN for the first 60 min in Mn^{2+} containing reactions, and $15.10 \pm 1.23 (\times 10^{-6})$ product copies generated per minute per molecule IN in Mg^{2+} containing reactions. IN is a sluggish enzyme *in vitro*, perhaps because it needs to carry out each reaction step only once *in vivo*. Turnover is very slow, but has been detected in specifically designed experiments (39).

The D64A IN did not convert any detectable substrate to product in either Mn^{2+} or Mg^{2+} . The D64C IN was able to generate disintegration product in the presence of Mn^{2+} , but not Mg^{2+} , indicating functional binding of the Mn^{2+} ion to the cysteine residue (Figure 3B). A time course for D64C showed that the initial rate of product conversion for D64C in the presence of Mn^{2+} was about $2.35 \pm 0.21 (\times 10^{-6})$ product copies generated per minute per molecule IN.

In the presence of the D116C there was a large increase in activity with Mn^{2+} , while no activity was detected with Mg^{2+} . For the D116A IN there was a low, but measurable, amount of product formed in the presence of Mn^{2+} (4- to 5-fold lower than the D116C IN at 4 h), but not in the presence of Mg^{2+} . This may indicate that D116 is not as critical for metal binding as the other two members of the catalytic triad. For several other members of the RNase H family, low levels of activity have also been seen with corresponding amino acid substitutions (12,14,22,40). The rate of product formation during a 60 min time course with Mn^{2+} was measured and the D116C IN was found to generate about $19.09 \pm 1.00 (\times 10^{-6})$ product copies per minute per molecule IN compared to about $1.79 \pm 0.14 (\times 10^{-6})$ product copies generated per minute per molecule IN for the D116A IN in the presence Mn^{2+} .

We next tested the E152A and E152C INs (Figure 3C), which previously had undetectable activity. The E152A IN showed no detectable activity in a 4 h disintegration reaction. The E152C IN, on the other hand, was able to produce product in the presence of Mn^{2+} , and not in the presence of Mg^{2+} , revealing functional metal binding by the cysteine residue. As seen in Figure 3D, there was increased product formed over time by the E152C enzyme in the presence of Mn^{2+} . The rate over the first 60 min was estimated at $0.564 \pm 0.058 (\times 10^{-6})$ product copies generated per minute per molecule IN, which is 1% the rate measured for the WT IN.

In order to verify that the product measured in E152C IN reactions was the expected transesterification product, we

amplified the reaction product using a radiolabeled Dis F primer instead of carrying out qPCR with the TaqMan probe. The PCR products were compared to a ^{32}P -labeled synthetic 97mer oligonucleotide matching the expected product (Figure 3E). The 97mer product comprised 70–90% of the detectable product in reactions containing WT IN in the presence of either metal cofactor. No product was seen for the E152A IN with either metal ion. For E152C IN, 90% of product was the expected 97mer and it was only detected in the presence of Mn^{2+} . The doublet seen for WT IN is either a PCR artifact, an artifact resulting from overloading the gel well or the result of a low level of transesterification involving another phosphodiester.

In the next sections, we present two further uses of the qPCR-based disintegration assay in studies of HIV IN. In the first, we show that transesterification by IN can involve a DNA 5' end as well as a 3' end. In the second, we detect catalysis in the presence of metal atoms only, allowing an initial estimation of the rate enhancement contributed by the protein scaffold of the IN enzyme.

WT IN activity on a substrate with reversed chemical polarity

In order to examine alternate transesterification reactions, we designed a new substrate (Figure 4A) in which an exposed 5' hydroxyl is present near the joining point of the 'target' and 'LTR' DNA analogs, rather than the standard 3' hydroxyl. In reactions with this reversed polarity substrate, product will be measurable only if the free 5' hydroxyl is able to act as a nucleophile for attacking the backbone to form the 97mer product. As seen in Figure 4B, the wild-type IN was able to generate product over time in the presence of Mn^{2+} on the reverse polarity substrate. Product was not observed in the presence of Mg^{2+} . The rate of product formation in the presence of Mn^{2+} was $1.07 \pm 0.14 (\times 10^{-6})$ product copies generated per minute per molecule IN, about 1% of the rate with WT IN. We also attempted to test the alanine and cysteine-substituted enzymes on this substrate. No activity was detected, indicating a lack of metal rescue (data not shown). This may be due to suboptimal positioning of the alternate substrate in the active site of IN confounded by the presence of amino acid substitutions, which alter the conformation of the active site.

DNA transesterification reactions in the absence of protein

In order to study the rate enhancement contributed by the IN-protein scaffold, we assayed disintegration in reactions containing metal ion cofactors without added protein catalyst. For these reactions we used the standard disintegration substrate and buffer conditions as used for IN reactions and compared different metals or no added metal (100 μM EDTA) in the absence of IN. We initially scanned a wide range of conditions, including comparing incubation at either 37 or 95°C for up to 24 h. In one test, reaction mixtures were dehydrated in a SpeedVac before heating at 95°C.

Dehydrated reactions mixtures incubated at 95°C produced measurable amounts of transesterification product (Figure 5). In contrast, 37°C incubation (either with or without dehydration) did not yield any detectable product (data not shown).

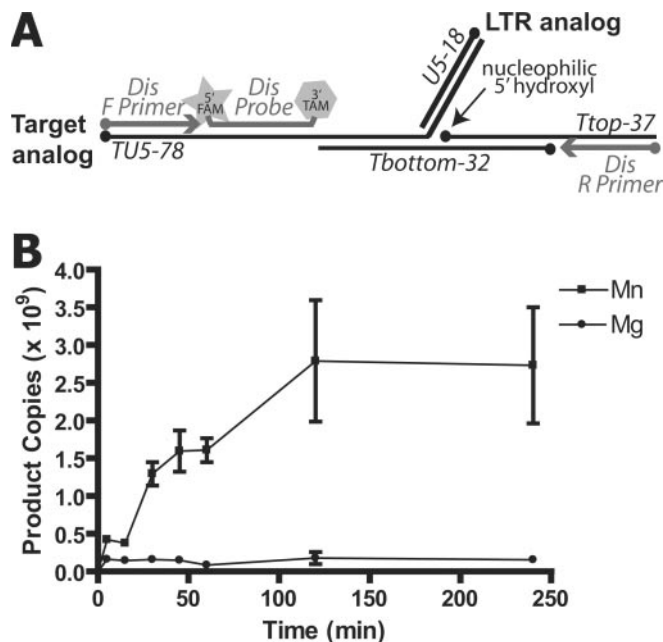


Figure 4. DNA transesterification activity of HIV-1 on a reverse polarity substrate. (A) Schematic of the reverse polarity substrate, which contains a free 5' hydroxyl at the DNA three-way junction in place of the usual 3' hydroxyl. The same primers and probe are used to measure product copies for the two substrates. The 5' ends are noted by black dots. (B) A time course for DNA transesterification activity of WT IN on the reversed polarity substrate in the presence of 10 mM MnCl₂ or 20 mM MgCl₂. Error bars indicate one standard deviation around the mean of qPCR performed in triplicate. To show that the difference seen between reactions with Mn²⁺ and Mg²⁺ were significantly different, three independent reactions from the 2 h time point (the time point for which we had the most replicates) with triplicate qPCR for each were compared using a one-tailed Mann-Whitney *U*-test ($P < 0.0001$).

Figure 5A shows an example of a time course carried out at 95°C in the presence of either 50 mM MnCl₂ or 100 μM EDTA. Product for the MnCl₂ reactions was distinguishable from the EDTA control reactions after 1 h of incubation, and continued product formation was seen up to 22 h in the presence of MnCl₂. We consistently saw a reduced rate of product generation at longer times, perhaps due to competing DNA degradation under the extreme conditions used. We also carried out assays under the same conditions in the presence of 50 mM MgCl₂, but no product was detected (data not shown). The product structure was characterized by PCR amplification with labeled primers, followed by electrophoresis on DNA-sequencing-type gels (Figure 5B). The product of the reaction in the presence of Mn²⁺ showed the expected 97mer length. Small amounts of product were detected in the EDTA control as well, but these were lower in abundance than the 50-copy standard and are of uncertain significance.

These measurements allow us to make an initial estimate of the rate enhancement in the disintegration reaction resulting from binding the metal atoms and DNA to the IN-protein scaffold. The reaction conditions in the presence and absence of IN are quite different, so the value represents an initial estimation of a lower limit. We compared the initial rate of product formation per minute between reactions at 37°C with 1 μM WT IN (first 60 min) and 10 mM MnCl₂ to reactions at 95°C with no IN and 50 mM MnCl₂ (first 180 min). For WT IN the rate of product copies generated per minute was

$1.23 \pm 0.18 (\times 10^9)$ and for the reactions without IN the rate of product copies generated per minute was $1.09 \pm 0.10 (\times 10^3)$. In order to account for the difference in temperature, we corrected by the temperature coefficient (Q_{10}), estimating a 2-fold increase in rate for every 10°C increase in temperature (41). Thus if the enzymatic reactions were carried out at 95°C (and the enzyme was still stable) the rate would be increased theoretically by a factor of 56, to 6.9×10^{10} product copies generated per minute. That indicates that the protein scaffold of the HIV-1 IN increased the rate of DNA transesterification by a factor of at least 60 million.

DISCUSSION

In this study, we present a sensitive and quantitative assay for measuring DNA transesterification reactions based on the disintegration reaction of retroviral INs. This was made possible by adding a TaqMan real-time PCR detection step, which was found to increase sensitivity at least 1000-fold over previous assays using radiolabeled substrates. We used the new method to investigate three issues surrounding the role of metal atoms in catalysis by HIV IN. These are discussed sequentially below.

Previously, our laboratory investigated the role of the conserved acidic residues of HIV-1 IN by monitoring metal rescue of cysteine substitutions (23). No activity was detected for E152C, leaving open the role of this residue. Similar studies have been carried out on other RNase H-like superfamily members, such as Tn7 TnsA (31), Tn10 transposase (28) and RAG1 (29,30). For Tn10, all three residues of the catalytic triad were found to coordinate metal ions, while the other studies only showed functional metal binding by metal rescue for one of the three residues. For the enzyme family more broadly, there has been debate over whether the enzymes utilize one or two metal mechanisms for catalysis (16,20,21). Thanks to the increased sensitivity provided by the real-time PCR step, we were able to observe metal rescue for the E152C IN (Figure 3C), as well as confirm rescue of the D64C and D116C INs (Figure 3B). As expected, product formation was not observed for the E152A IN with either metal ion and no product was formed with E152C IN in the presence of the Mg²⁺. The activity with E152C in Mn²⁺ was only 1% that of WT IN, but the specificity for the cysteine versus the alanine residue and Mn²⁺ versus Mg²⁺ metal supports the idea that E152 is normally involved in metal binding. The activity of E152C IN may have been reduced compared to wild-type IN because the E152 side chain makes additional contacts besides binding to a single metal atom and/or because the cysteine side chain is shorter than that of glutamate, potentially resulting in suboptimal positioning of the metal atom in the active site. These results support the model shown in Figure 3A, where all three catalytic residues coordinate the binding of two metal ions that carry out catalysis, and argue against the idea that the second metal might be inhibiting catalysis. We disfavor the view that all three acidic residues bind a single metal ion, since that would be inconsistent with the geometry in Figure 3A. Because IN-protein is does not turnover efficiently *in vitro* and is not amenable to detailed kinetic analysis, it has not been possible to assign the effects of metal atoms to specific

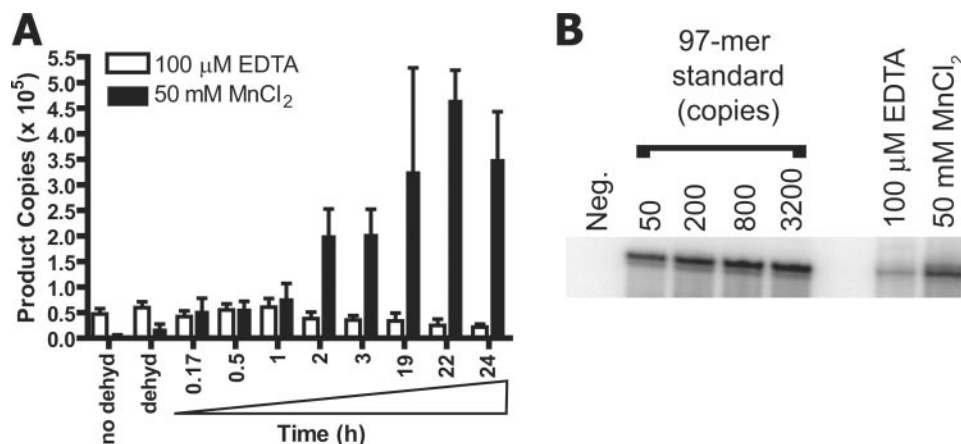


Figure 5. DNA transesterification reactions in the presence of Mn²⁺ alone. DNA transesterification reactions were carried out on the standard substrate in the absence of IN. (A) Reactions with 50 mM MnCl₂ or 100 μM EDTA were not treated ('no dehyd') or dehydrated in a SpeedVac ('dehyd') followed by heating for the indicated amount of time at 95°C and 1/100 dilutions were analyzed by qPCR. The total product copies generated during the transesterification reaction are graphed. Error bars indicate one standard deviation around the mean of two independent transesterification reactions each analyzed in triplicate by qPCR. The difference between the reactions with Mn²⁺ versus EDTA was compared for each time point and found to be significant with a *P*-value of 0.0011, based on a one-tailed Mann-Whitney *U*-test, for all time points after 1 h. (B) Verification of the sizes of reaction products by PCR amplification with end-labeled primer and 8% denaturing gel electrophoresis. Products for PCRs containing 10-fold dilutions of reactions from the 22 h time point were compared to amplifications of the 97mer oligonucleotide representing reaction product and used in the standard curve. The number of copies of 97mer standard added is indicated above the autoradiogram.

steps in the reaction pathway. Thus strictly speaking, complicated models are not ruled out in which the Cys-metal complexes in the rescue experiments are acting differently than the carboxyl-metal complexes in wild-type IN. However, together with the results on the Tn7 and Tn10 transposases, these results are most simply interpreted as evidence that IN/transposase enzymes of the RNase H-like superfamily probably all use two divalent metal ions for catalysis.

We also used the qPCR-based assay to examine catalysis on a reverse polarity substrate, which has a free 5' hydroxyl at the junction of target DNA and the LTR end instead of a 3' hydroxyl. The wild-type HIV-1 IN was capable of catalyzing a DNA transesterification reaction on this substrate in the presence of Mn²⁺, but not in the presence of Mg²⁺. In attempted metal rescue experiments, no activity was detected for any of the cysteine-substituted INs with either Mn²⁺ or Mg²⁺. Possibly incorrect positioning of the substrate within the enzyme active site made it difficult for the enzyme to act in the presence of further impaired enzyme/metal combinations. Whether this reaction has any biological role is unknown. The finding that a 5' hydroxyl can be recruited by IN to participate in transesterification adds to the surprisingly wide range of hydroxylated compounds reported to function as nucleophiles in the presence of Mn²⁺, including 3' hydroxyls of various nucleotides and a variety of vicinal alcohols (42–46).

The increased sensitivity of the qPCR-based assay also provides a convenient and quantitative method for investigating novel catalysts of DNA transesterification reactions. Here, we investigated metal-mediated catalysis in the absence of a protein enzyme. Previously, it was suggested that, for enzymes binding two metals, the metal atoms may be responsible for most of the catalytic contacts in the transition state, while the protein serves to bind and orient the metals and substrates (2). According to this idea, it might be possible to detect transesterification in the presence of high concentrations of metals

with a sufficiently sensitive assay. We subjected the standard substrate presented here (Figure 1B, upper) to high metal concentrations, high temperature and dehydration, which allowed detection of amplifiable product. The reaction required Mn²⁺, since product accumulation over time was only detected in reactions containing Mn²⁺, and not Mg²⁺ or EDTA.

The detection of low level transesterification in the presence of Mn²⁺ only allowed us to make a first estimation of the rate enhancement due to binding metal and reactant DNAs to the IN-protein scaffold. In previous studies of staphylococcal nuclease, the spontaneous hydrolysis rate of phosphodiester was measured with chemical models, allowing the rate enhancement by the enzyme to be estimated as a factor of 10¹⁷ (47). Here we estimate that the rate enhancement of IN plus Mn²⁺ over Mn²⁺ alone is a factor of at least 60 million. This estimate is a lower bound, because the reactions were carried out under quite different conditions. For example, it is possible that the polypropylene surface of the microcentrifuge tube on which the Mn²⁺-only reaction took place played a role, as has been proposed for mineral surfaces in pre-biotic chemistry (48,49). If so, the spontaneous rate in the absence of IN would be even lower. Further optimization of conditions for both the IN-catalyzed and Mn²⁺-alone reactions could also influence the measured difference in rate. Despite these uncertainties, this estimation of the rate enhancement provides new information potentially useful for quantitative modeling of active site function.

Lastly, we note that the qPCR-based disintegration assay is potentially useful for a wide range of applications that require sensitive detection of transesterification products. The RAG-1 recombinase and several bacterial transposases are known to carry out disintegration reactions, so the qPCR-based method can be used to study mutants or reaction conditions supporting only low level activity of these enzymes. The new assay also provides a method for screening candidate small molecule inhibitors of IN or other enzymes

using very low amounts of reactants, made possible by the sensitive detection method. Finally, the qPCR-based assay also provides a sensitive means for scanning candidate catalysts to identify possible reactions important in pre-biotic nucleic acid chemistry.

ACKNOWLEDGEMENTS

The authors thank members of the Bushman laboratory for helpful discussions. This work was supported by NIH grant GM068408, the James B. Pendleton Charitable Trust and Robin and Frederic Withington. T.L.D. is a fellow of The Leukemia and Lymphoma society (5217-06). Funding to pay the Open Access publication charges for this article was provided by NIH grant GM068408.

Conflict of interest statement. None declared

REFERENCES

- Beese, L.S. and Steitz, T.A. (1991) Structural basis for the 3'-5' exonuclease activity of *Escherichia coli* DNA polymerase I: a two metal ion mechanism. *EMBO J.*, **10**, 25–33.
- Steitz, T.A. and Steitz, J.A. (1993) A general two-metal-ion mechanism for catalytic RNA. *Proc. Natl Acad. Sci. USA*, **90**, 6498–6502.
- Pan, T., Long, D.M. and Uhlenbeck, O.C. (1993) Divalent metal ions in RNA folding and catalysis. In Gesteland, R.F. and Atkins, J.F. (eds), *The RNA World*. Cold Spring Harbor Laboratory Press, Cold Spring Harbor, NY, pp. 271–302.
- Rice, P., Craigie, R. and Davies, D.R. (1996) Retroviral integrases and their cousins. *Curr. Opin. Struct. Biol.*, **6**, 76–83.
- Yang, W. and Steitz, T.A. (1995) Recombining the structures of HIV integrase, RuvC, and RNase H. *Structure*, **3**, 131–134.
- Yang, Z.N., Mueser, T.C., Bushman, F.D. and Hyde, C.C. (2000) Crystal structure of an active two-domain derivative of rous sarcoma virus integrase. *J. Mol. Biol.*, **296**, 535–548.
- Dyda, F., Hickman, A.B., Jenkins, T.M., Engelman, A., Craigie, R. and Davies, D.R. (1994) Crystal structure of the catalytic domain of HIV-1 integrase: similarity to other polynucleotidyl transferases. *Science*, **266**, 1981–1986.
- Bujacz, G., Alexandratos, J., Wlodawer, A., Merkel, G., Andrade, M., Katz, R.A. and Skalka, A.M. (1997) Binding of different divalent cations to the active site of avian sarcoma virus integrase and their effects on enzymatic activity. *J. Biol. Chem.*, **272**, 18161–18168.
- Bujacz, G., Jaskolski, M., Alexandratos, J., Wlodawer, A., Merkel, G., Katz, R.A. and Skalka, A.M. (1996) The catalytic domain of avian sarcoma virus integrase: conformation of the active-site residues in the presence of divalent cations. *Structure*, **4**, 89–96.
- Bushman, F.D. (2001) *Lateral DNA Transfer: Mechanisms and Consequences*. Cold Spring Harbor Laboratory Press, Cold Spring Harbor, NY.
- Craig, N.L., Craigie, R., Gellert, M. and Lambowitz, A.M. (2002) *Mobile DNA II*. ASM Press.
- Nowotny, M., Gaidamakov, S.A., Crouch, R.J. and Yang, W. (2005) Crystal structures of RNase H bound to an RNA/DNA hybrid: substrate specificity and metal-dependent catalysis. *Cell*, **121**, 1005–1016.
- Davies, J.F., Hostomska, Z., Hostomsky, Z., Jordan, S.R. and Matthews, D.A. (1991) Crystal structure of the ribonuclease H domain of HIV-1 reverse transcriptase. *Science*, **252**, 88–95.
- Nowotny, M. and Yang, W. (2006) Stepwise analyses of metal ions in RNase H catalysis from substrate destabilization to product release. *EMBO J.*, **25**, 1924–1933.
- Goldgur, Y., Dyda, F., Hickman, A.B., Jenkins, T.M., Craigie, R. and Davies, D.R. (1998) Three new structures of the core domain of HIV-1 integrase: an active site that binds magnesium. *Proc. Natl Acad. Sci. USA*, **95**, 9150–9154.
- Katayanagi, K., Okumura, M. and Morikawa, K. (1993) Crystal structure of *Escherichia coli* RNase HI in complex with Mg²⁺ at 2.8 Å resolution: proof for a single Mg(2+)-binding site. *Proteins*, **17**, 337–346.
- Lubkowski, J., Yang, F., Alexandratos, J., Wlodawer, A., Zhao, H., Burke, T.R.J., Neamati, N., Pommier, Y., Merkel, G. and Skalka, A.M. (1998) Structure of the catalytic domain of avian sarcoma virus integrase with a bound HIV-1 integrase-targeted inhibitor. *Proc. Natl Acad. Sci. USA*, **95**, 4831–4836.
- Maignan, S., Guilloteau, J.P., Zhou-Liu, Q., Clement-Mella, C. and Mikol, V. (1998) Crystal structures of the catalytic domain of HIV-1 integrase free and complexed with its metal cofactor: High level of similarity of the active site with other viral integrases. *J. Mol. Biol.*, **282**, 359–368.
- Tsunaka, Y., Takano, K., Matsumura, H., Yamagata, Y. and Kanaya, S. (2005) Identification of single Mn(2+) binding sites required for activation of the mutant proteins of *E.coli* RNase HI at Glu48 and/or Asp134 by X-ray crystallography. *J. Mol. Biol.*, **345**, 1171–1183.
- Black, C.B. and Cowan, J.A. (1994) Magnesium activation of ribonuclease H. Evidence for one catalytic metal ion. *Inorg. Chem.*, **33**, 5805–5808.
- Lai, B., Li, Y., Cao, A. and Lai, L. (2003) Metal ion binding and enzymatic mechanism of *Methanococcus jannaschii* RNase HIII. *Biochemistry*, **42**, 785–791.
- Keck, J.L., Goedken, E.R. and Marqusee, S. (1998) Activation/attenuation model for RNase H. A one-metal mechanism with second-metal inhibition. *J. Biol. Chem.*, **273**, 34128–34133.
- Gao, K., Wong, S. and Bushman, F. (2004) Metal binding by the D,DX35E motif of human immunodeficiency virus type 1 integrase: selective rescue of Cys substitutions by Mn²⁺ *in vitro*. *J. Virol.*, **78**, 6715–6722.
- Gordon, P.M., Sontheimer, E.J. and Piccirilli, J.A. (2000) Metal ion catalysis during the exon-ligation step of nuclear pre-mRNA splicing: extending the parallels between the spliceosome and group II introns. *RNA*, **6**, 199–205.
- Houglund, J.L., Kravchuk, A.V., Herschlag, D. and Piccirilli, J.A. (2005) Functional identification of catalytic metal ion binding sites within RNA. *PLoS Biol.*, **3**, e277.
- Sontheimer, E.J., Sun, S. and Piccirilli, J.A. (1997) Metal ion catalysis during splicing of premessenger RNA. *Nature*, **388**, 801–805.
- Yoshida, A., Sun, S. and Piccirilli, J.A. (1999) A new metal ion interaction in the Tetrahymena ribozyme reaction revealed by double sulfur substitution. *Nature Struct. Biol.*, **6**, 318–321.
- Allingham, J.S., Pribil, P.A. and Hanford, D.B. (1999) All three residues of the Tn 10 transposase DDE catalytic triad function in divalent metal ion binding. *J. Mol. Biol.*, **289**, 1195–1206.
- Kim, D.R., Dai, Y., Mundy, C.L., Yang, W. and Oettinger, M.A. (1999) Mutations of acidic residues in RAG1 define the active site of the V(D)J recombinase. *Genes Dev.*, **13**, 3070–3080.
- Landree, M., Wibbenmeyer, J. and Roth, D. (1999) Mutational analysis of RAG1 and RAG2 identifies three catalytic amino acids in RAG1 critical for both cleavage steps of V(D)J recombination. *Genes Dev.*, **13**, 3059–3069.
- Sarnovsky, R.J., May, E.W. and Craig, N.L. (1996) The Tn7 transposase is a heteromeric complex in which DNA breakage and joining activities are distributed between different gene products. *EMBO J.*, **15**, 6348–6361.
- Soundar, S., O'Hagan, M., Fomulu, K.S. and Colman, R.F. (2006) Identification of Mn²⁺-binding aspartates from alpha, beta and gamma subunits of human NAD-dependent isocitrate dehydrogenase. *J. Biol. Chem.*, **281**, 21073–21081.
- Curley, J.F., Joyce, C.M. and Piccirilli, J.A. (1997) Functional evidence that the 3'-5' exonuclease domain of *Escherichia coli* DNA polymerase I employs a divalent metal ion in leaving group stabilization. *J. Am. Chem. Soc.*, **119**, 12691–12692.
- Chow, S.A., Vincent, K.A., Ellison, V. and Brown, P.O. (1992) Reversal of integration and DNA splicing mediated by integrase of human immunodeficiency virus. *Science*, **255**, 723–726.
- Melek, M. and Gellert, M. (2000) RAG1/2-mediated resolution of transposition intermediates: two pathways and possible consequences. *Cell*, **101**, 625–633.
- Au, T.K., Pathania, S. and Harshey, R.M. (2004) True reversal of Mu integration. *EMBO J.*, **23**, 3408–3420.
- Gao, K., Butler, S.L. and Bushman, F.D. (2001) Human immunodeficiency virus type 1 integrase: arrangement of protein domains in active cDNA complexes. *EMBO J.*, **20**, 3565–3576.

38. Diamond, T.L. and Bushman, F.D. (2005) Division of labor within human immunodeficiency virus integrase complexes: determinants of catalysis and target DNA capture. *J. Virol.*, **79**, 15376–15387.
39. Chow, S.A. and Brown, P.O. (1994) Substrate features important for recognition and catalysis by human immunodeficiency virus type 1 integrase identified by using novel DNA substrates. *J. Virol.*, **68**, 3896–3907.
40. Kanaya, S., Kimura, S., Katsuda, C. and Ikehara, M. (1990) Role of cysteine residues in ribonuclease H from *Escherichia coli*. Site-directed mutagenesis and chemical modification. *Biochem. J.*, **271**, 59–66.
41. Lehninger, A. (1979) *Biochemistry*. 2nd edn. Worth Publishers, New York, NY.
42. Engelman, A., Mizuuchi, K. and Craigie, R. (1991) HIV-1 DNA integration: mechanism of viral DNA cleavage and DNA strand transfer. *Cell*, **67**, 1211–1221.
43. van Gent, D.C., Oude Groneneger, A.A.M. and Plasterk, R.H.A. (1993) Identification of amino acids in HIV-2 integrase involved in site-specific hydrolysis and alcoholysis of viral DNA termini. *Nucleic Acids Res.*, **21**, 3373–3377.
44. Skinner, L.M., Sudol, M., Harper, A.L. and Katzman, M. (2001) Nucleophile selection for the endonuclease activities of human, ovine, and avian retroviral integrases. *J. Biol. Chem.*, **276**, 114–124.
45. Katzman, M. and Sudol, M. (1996) Nonspecific alcoholysis, a novel endonuclease activity of human immunodeficiency virus type 1 and other retroviral integrases. *J. Virol.*, **70**, 2598–2604.
46. Vink, C., Yeheskiely, E., van der Marel, G.A., van Boom, J.H. and Plasterk, R.H.A. (1991) Site-specific hydrolysis and alcoholysis of human immunodeficiency virus DNA termini mediated by the viral integrase protein. *Nucleic Acids Res.*, **19**, 6691–6698.
47. Schroeder, G.K., Lad, C., Wyman, P., Williams, N.H. and Wolfenden, R. (2006) The time required for water attack at the phosphorus atom of simple phosphodiester and of DNA. *Proc. Natl Acad. Sci. USA*, **103**, 4052–4055.
48. Ferris, J.P., Hill, A.R., Jr, Liu, R. and Orgel, L.E. (1996) Synthesis of long prebiotic oligomers on mineral surfaces. *Nature*, **381**, 59–61.
49. Orgel, L.E. (1998) Polymerization on the rocks: theoretical introduction. *Orig. Life Evol. Biosph.*, **28**, 227–234.